

SYNTHESIS OF SILVER NANOSPHERES AND NANOBARS BY HYDROTHERMAL PROCESS

Phan Ha Nu Diem

Hue University

ABSTRACT

Small silver nanospheres and nanobars have been prepared using hydrothermal process. Thermogenetic magnetic stirred machine treatment of the mixture of silver nitrate and sodium borohydride in the presence of trisodium citrate in aqueous. Results in the formation of poorly crystallized silver at ambient temperature. As a result, we were able to achieve a nucleation burst in the early stage to generate a large number of seeds and a relatively slow growth rate thereafter. Silver nanobars with rectangular side facets and an average aspect ratio of 3 have been synthesized by modifying feeding speed of reactants. Due to their anisotropy, Ag nanobars exhibit two plasmon resonance peaks. The microstructure of Ag nanospheres and nanobars was tested by XRD and TEM. The different growth process of Ag nanospheres and nanobars has been traced by UV – visible absorption spectra. It is shown that the silver nanospheres and nanobars prepared of in aqueous solution through adequate reaction temperature, concentrations of AgNO_3 and NaBH_4 solutions, feeding speed of reactants... possess well compositional homogeneity and different morphologies.

1. INTRODUCTION

Over the past decade or so, silver nanocrystals have been a subject of intensive researches. They exhibit remarkable physicochemical and optical properties, which are not observed neither in molecules nor in bulk metals. The field of biomedicine using silver nanoparticles is appealing due to their broadacting biocidal activities and unique plasmonics properties in the visible region [1], [2], [3].

For biomedical applications, watersoluble Ag nanoparticles are highly desirable. Nowadays, Ag nanoparticles can be synthesized using various methods: chemical [3], γ -radiation [4], photochemical [5] etc. Therein, the most popular preparation of Ag

colloids is chemical reduction of silver salts by sodium borohydride in the presence of sodium citrate solution in aqueous. Controllable synthesis of AgNPs in aqueous solution still remains a challenging task due to the hard to control nucleation process arising from the high reactivity of silver precursors in water [3], [6].

New thoughts for this method relies on the modification of feeding speed AgNO_3 and NaBH_4 solutions. This solutions were simultaneously injected drop – wise (finish injecting in about 10 min). AgNO_3 solution has been completely consumed by NaBH_4 , the Ag nanocrystals can not grow into large sizes although Ag nanocrystals possess the intrinsic autocatalytic activity. Ag nanobars

could be synthesized by this process with the edge lengths are sub 20nm. Small nanostructures with tunable SPR properties are expected to show enhanced performance in a number of in vivo applications that include drug delivery, optical imaging, and photothermal therapy.

The purity of water and reagents, cleanliness of the glassware are critical parameters.

2. MATERIALS AND METHODS

Silver nitrate (AgNO_3), sodium borohydride (NaBH_4), trisodium citrate dihydrate ($\text{C}_6\text{H}_5\text{Na}_3\text{O}_7 \cdot 2\text{H}_2\text{O}$) were all obtained from Sigma – Aldrich. Twice distilled water was used throughout the total experiments. The standard synthesis of Ag nanocrystals was carried out in a 100 mL three – necked round bottom flask equipped with a reflux condenser. All the glassware was cleaned by aqua regia ($\text{HCl}:\text{HNO}_3$ in a 3:1 ratio by volume) and rinsed with deionized water prior to the experiments.

Reaction products were identified by an X-ray diffractory (XRD) (Rikaku- Denki, $\text{CuK}\alpha$, 40 mV, 20 mA). The morphology of silver nanocrystal were observed in a UV-visible extinction spectra were recorded by a Shimadzu UV-630 spectrophotometer and an transmission electron microscopy (TEM) images were taken using a Hitachi H-7500 microscope operated at 75 kV.

The synthesis method of silver nanocrystal based on thoughts of science material [3]. 5 mL of 1% citrate solution and 19 mL of water were added in a round bottom flask and the mixture was heated under magnetic stirring in an oil bath set at different temperatures for 15 min. Other reagents were separately dissolved in twice distilled water and sequentially introduced into the flask using a pipet. Specifically, 0.43 mL of 1% AgNO_3 solution was introduced to the mixture, followed by the quick addition of 0.5 mL of 0.1% freshly prepared NaBH_4 cool solution. The reaction solution was kept at 70°C under vigorous stirring for 1h. During the entire process, stirring continued while keeping reflux, the flask was capped with glass stoppers except for the addition of reagents. The synthesis was quenched by placing the three – necked round bottom flask in an ice – water bath. (table 1)

Table. 1: The samples were synthesis at different temperatures

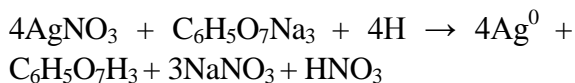
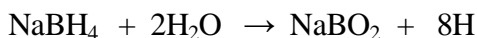
Sample	V_{Citrate} (mL)	V_{Water} (mL)	$V_{\text{Silver nitrate}}$ (mL)	$V_{\text{Sodium borohydride}}$ (mL)	Hydrothermal temperature ($^\circ\text{C}$)
1a	5	19	0.43	0.5	110
1b	5	19	0.43	0.5	ambient
1d	5	19	0.43	0.5	70

Different from the aforementioned procedure, AgNO_3 and NaBH_4 solution were simultaneously injected drop - wise (finish injecting in about 5 min). The reaction solution was kept at 70°C under vigorous stirring for 1h. (table 2).

Table. 2: The samples were prepared from different injected methods

Sample	$V_{\text{Citrate 1\%}}$ (mL)	V_{Water} (mL)	AgNO_3		NaBH_4		AgNO_3 and NaBH_4 were simultaneously injected
			$V_{\text{(mL)}}$	C%	$V_{\text{(mL)}}$	C%	
M_1	5	0	8.5	0.05	10	0.005	10 min
M_2	5	15	1.7	0.25	2.0	0.025	10 min
M_3	5	15	1.7	0.25	2.0	0.025	5 min

In the presence of metal catalysts, sodium borohydride releases hydrogen. The hydrogen is generated by decomposition of the aqueous borohydride solution. Exploiting this reactivity, sodium borohydride is used in synthesis of metal nanoparticles. Hydrogen atoms used throughout the total experiments were prepared by sodium borohydride dissolves in refrigerated water, mechanism of reaction could be expressed as follows:



3. RESULTS AND DISCUSSION

This procedure begins with the synthesis of metallic nanoparticles by chemical reduction of a metal salt with a strong reducing agent such as sodium borohydride. Citrate is present as a capping agent to prevent particle growth. Reaction temperature was found to play an important role in the preparation of silver nanoparticles (Figure 1A).

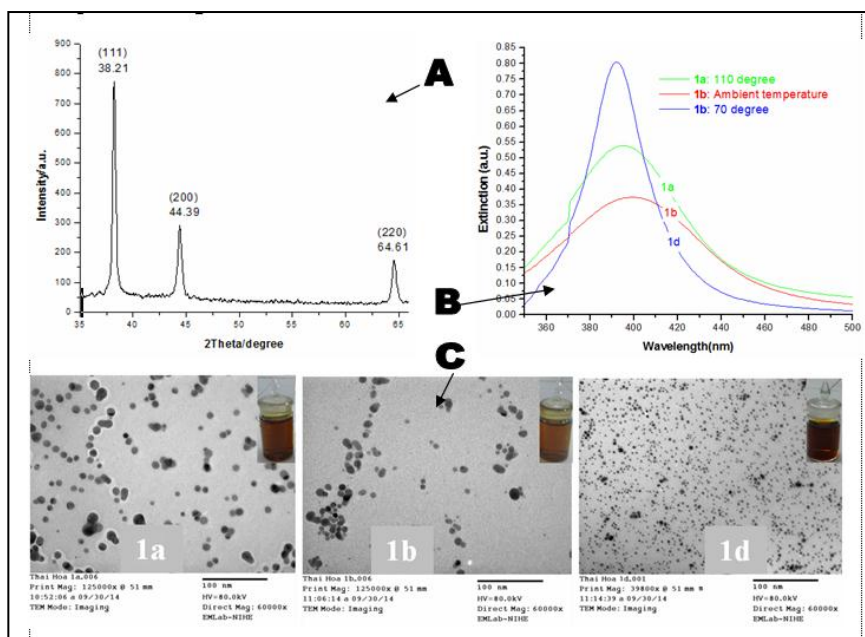


Figure 1. Demonstration of the synthesis of small Ag nanospheres by reaction temperature investigation: (A) UV-vis spectra of three different batches of Ag nanoparticles shown in (C), which had different sizes. (B) XRD pattern of silver nanoparticles. (C) TEM images showing size of Ag nanoparticles were synthesised at different temperatures.

Shows the normalized UV-vis extinction spectra recorded from the silver nanospheres that were obtained at different reaction temperatures and the red brown solution of the resultant are manifests of characteristic surface plasmon resonance (SPR) of the silver nanospheres. The major SPR peaks displayed at 390, 395 and 399 nm positions correspond to 1d, 1a and 1b samples as the

size of the increased nanoparticles. As the reaction proceeds at 70°C, the intensity of this peak almost twice and the peak became narrower, indicating an increase in the number of Ag nanoparticles in the reaction solution and the uniformity of nanospheres compared with those at ambient temperature. Corresponding TEM images shows that these silver nanospheres were obtained at 70°C, the

sharp extinction 390 nm, the silver spheres thus generated are 4 ± 2 nm in diameter (Figure 1C). But over-high temperatures seemed to favor the formation of a large average size of Ag nanospheres with a broad size distribution was observed. When the reaction temperature increased to 110°C , most of the silver products were irregular nanospheres (14 ± 8 nm). To further confirm, the X-ray diffraction pattern of the silver nanospheres synthesized by hydrothermal method is shown in Figure 1B. Indexing process of powder diffraction pattern is done and *Miller Indices* (hkl) to each peak is assigned in first step (the details are in Table 3). A number of strong Bragg reflections can be seen which correspond to the (111), (200) and (220) reflections of face centered cubic (FCC) silver. No spurious diffractions due to crystallographic impurities are found [7]. Like this, no any spurious diffraction which indicating the crystallographic impurities in the sample. All the reflections correspond to pure silver metal with FCC symmetry. The high intense peak for FCC materials is generally (111) reflection, which is observed in the sample. The intensity of peaks reflected the high degree of crystallinity of the silver nanoparticles. However, the diffraction peaks are broad which indicating that the crystallite size is very small [8]. The XRD shows that silver nanoparticles formed are crystalline.

Table.3: Peak indexing from *d* – spacing

2θ	<i>d</i>	$1000/d^2$	$(1000/d^2)/60,62$	hkl
38.21	2.35	181.10	3	111
44.39	2.03	241.72	4	200
64.61	1.44	482.30	8	220

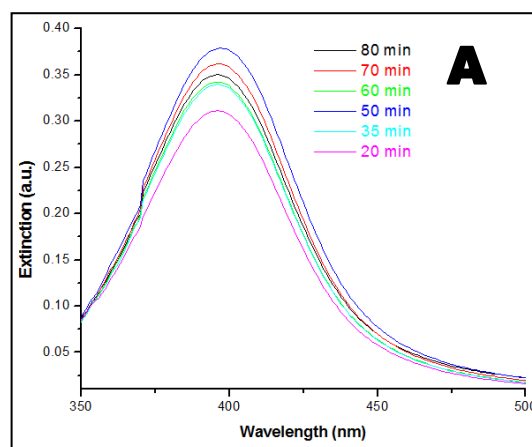
Three peaks at 2θ values of 38.21, 44.39 and 64.61 degree corresponding to (111), (200) and (220) planes of silver is observed and compared with the standard powder diffraction card of Joint Committee on

Powder Diffraction Standards (JCPDS), silver file No. 04–0783. The XRD study confirms that the resultant particles are (FCC) silver nanoparticles. [9]. The experimental diffraction angle $[2\theta]$ and standard diffraction angle $[2\theta]$ of the Table 4 are in agreement [10].

Table. 4: Experimental and standard diffraction angles of silver specimen

Experimental diffraction angle $[2\theta]$ in degrees]	standard diffraction angle $[2\theta]$ in degrees] JCPDS silver: 04–0783
44.39	44.3

A reactionist time investigation for synthesis of silver nanoparticles. As the reaction time increased, the intensity of this peak gradually increase (Figure 2A). At the reaction time is 50 minutes, the SPR peak of Ag nanoparticles obtained was the highest, resonant wavelength was invariable, suggesting that the concentration of Ag atoms should steadily increase. After the injection of Ag precursor, which is reduced and depleted in the presence of a reductant. If nucleation is allowed to proceed over an extended period, the precursor will be unevenly depleted, resulting in different growth rates for the nuclei formed at different stages of a synthesis. Corresponding TEM images shows that these silver nanoparticles were obtained at different time points (Figure 2B).



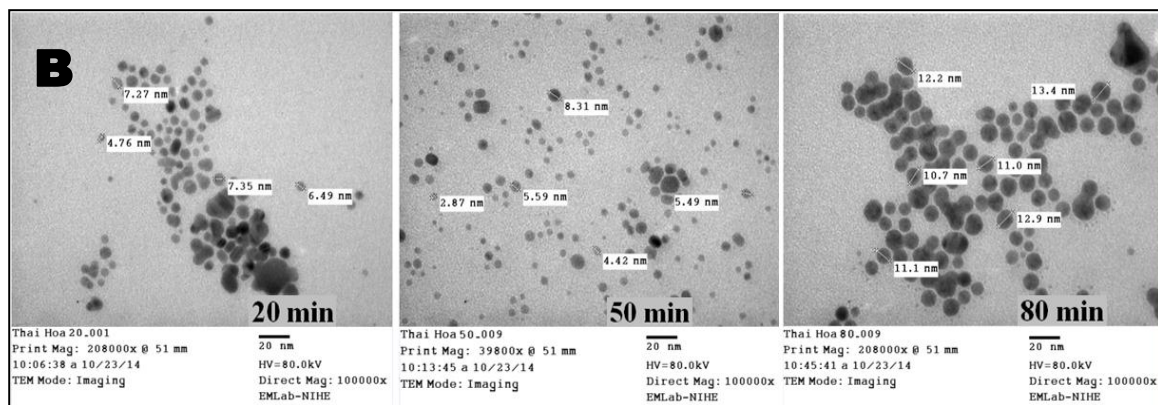
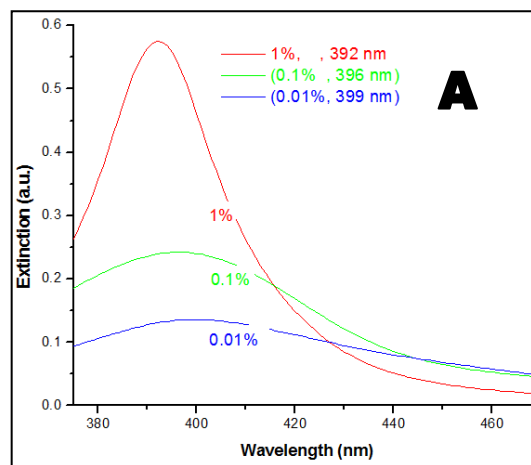


Figure 2. (B) Exhibit of Ag nanoparticle sizes in a reactionist time investigation. (A) UV–vis spectra of Ag nanoparticles obtained at different time points. (B) TEM images showing the stages of synthesis of Ag nanoparticles at 20, 50 and 80 minutes.

These arguments suggest that an effective approach to the synthesis of Ag nanocrystals with uniform sizes and shapes and in high purity is to separate the nucleation and growth steps. Consequently, we selected optimum reaction time was 50 minutes for following experiments.

We also optimized the synthesis by a AgNO_3 concentration investigation at three degree 0.01, 0.1 and 1% while other parameters were kept the same as the standard procedure. After the addition of NaBH_4 reduction, the colorless solution become yellowish color for solution had 0.01% Ag precursor concentration, suggesting that a forming of nucleation occurred. The products showed that their difference in AgNO_3 concentration could be a major parameter responsible for the small size, good uniformity and distribution of the Ag nanoparticles. After 50 minutes reaction, the precursor will be unevenly depleted, we placed the flask in an ice–water bath to slow growth of the seeds in the following step of the synthesis to allow for quenching. A small amount, 0.1 and 1.0 mL of the reaction solution corresponding to solution used Ag precursor concentration is 1 and 0.1% was

taken out from the flask using a glass pipet and were separately diluted with 10 mL twice distilled water in two phials. Figure 3A shows the normalized UV–vis extinction spectra recorded from aqueous suspensions of the Ag nanoparticles with Ag precursor concentration at 1, 0.1 and 0.01%. The major SPR peaks displayed a constant red-shift from 392 to 396 and 399 nm as the size of the nanoparticles increased, corresponding TEM images shows in figure 3B. The synthesis of Ag nanospheres was carried out in 1% AgNO_3 solution, the peak became narrower and the intense of this peak



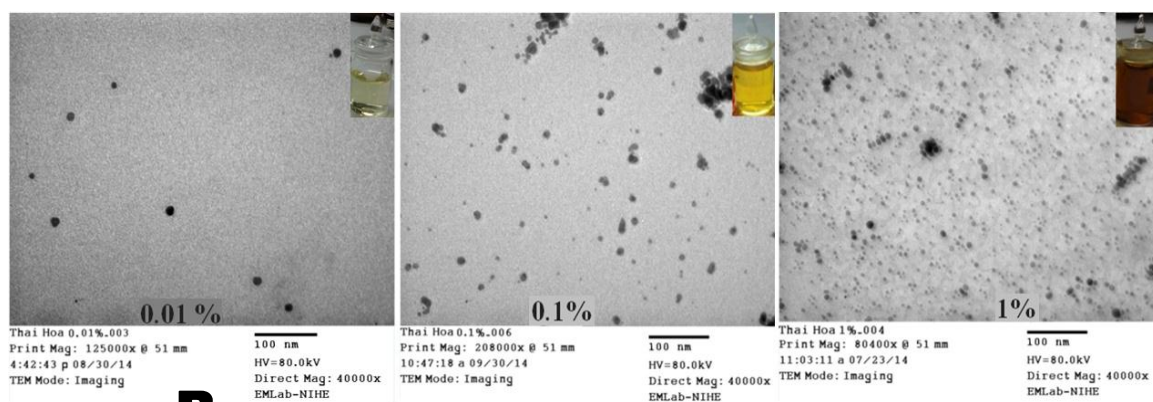


Figure 3. Demonstration of AgNO_3 concentrated exploration: (A) UV–vis spectra of Ag nanoparticles obtained at different AgNO_3 concentrated. (B) TEM images of the Ag nanoparticles obtained at 0.01, 0.1 and 1% AgNO_3 solution.

Almost triple compared with those at 0.1%, indicating an increase in the number of Ag nanoparticles in the reaction solution.

It is hard to understand why overthin Ag precursor concentration generated Ag seeds possess non-uniform and big size. Thus, feeding speed power of AgNO_3 and NaBH_4 is expected to play important role in the nucleation and growth. Therefore, we has to optimize several parameters such as the concentration of precursor, the reaction temperature and time to keep on an investigation of feeding speed reactants. Table 2 reveal M_1 , M_2 and M_3 samples possess the same AgNO_3 equilibrium concentration (0.425%), though they were different initial concentration. It is shown that the morphology of Ag nanoparticles is influenced by feeding speed of AgNO_3 and NaBH_4 (method section for details) as shown by TEM images in figure 4B. From the M_3 TEM image evidences that we were able to generate small silver nanobars in a aqueous medium about 16 ± 3 nm in long edge length, that possess rectangular side facets and an average aspect ratio of 3 have been synthesized by modifying feeding speed of reactants.

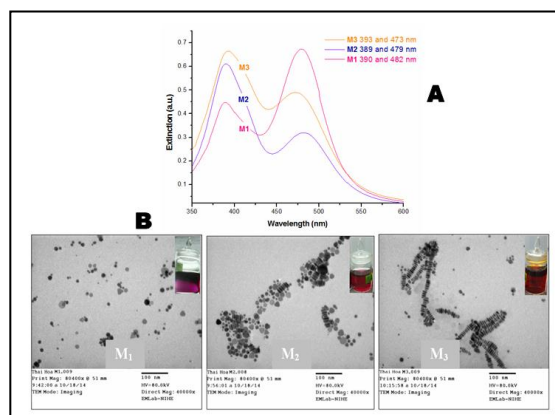


Figure 4. Shown that the morphology of Ag nanoparticles is influenced by feeding speed of AgNO_3 and NaBH_4 A) UV–vis spectra of three different batches of Ag nanoparticles as in 5 min (M_3) and 10 min (M_2) (as marked on the spectra). B) TEM images taken from aqueous suspensions of the Ag nanoparticles respectively A.

The M_3 spectrum exhibits two sharp peaks at 393 and 473 nm positions, and the red wine solution are expected to manifests of characteristic SPR of the Ag nanobars (Figure 4A). Therefore, we proceed to inhibiting each aforementioned peak to generation a perfect result. After experimental investigation, we achieved M_1 dark purple solution has two sharp SPR peaks at 390 and 482 nm positions of the resultant. Where, the intensity of 482 nm

peak almost twice compared with intensity at 390 nm peak. Besides, M_2 purple wine solution has two peaks at 389 and 479 nm. Conversely, the intensity of 389 nm peak is twice compared with intensity at 479 nm peak. Correspondence to TEM images (figure 4B), the final product was a mixture of rods, sheets and spheres with the same major sizes of 15 ± 5 nm.

It is not hard to understand why uniform Ag nanorods could be obtained in high yield in M_3 . It was because the low ratio of trisodium citrate to silver nitrate caused a decrease in coverage for the fast-growing end faces, and the incomplete coverage of trisodium citrate on end faces made nanorods grow longer. Therefore, M_3 suspension solution of almost silver nanorods and very little nanoparticles. On the contrary, the M_1 and M_2 structural systems are irregular, the yields of silver nanoparticles in that became lower and lower during the process with increasing the molar ratio of trisodium citrate to silver nitrate. The reason may be that the high ratio of trisodium citrate to silver nitrate might cause a relatively high coverage of trisodium citrate on every faces of nucleations (including fast-growing end faces and side surfaces), leading to an isotropic growth mode of silver nano-

particles. So the nanorods grew slower and shorter, and more nanospheres appeared.

4. CONCLUSIONS

Size, shape and morphology of the silver nanoparticles not only strongly depended on reaction temperature, time and Ag precursor concentration but also reactants injected speed. The silver nanoparticles were prepared by specifically injected method: silver nitrate and sodium borohydride solution, respectively at ambient temperature or on boiling were large average size about 14 ± 8 nm in diameter with a broad size distribution. When the reaction solution was kept heating at 70°C , the silver nanoparticles has a narrow size distribution of small average size about 4 ± 2 nm. If silver nitrate and sodium borohydride solution were simultaneously injected drop-wise about 5 minutes, we achieve a suspension solution of almost silver nanorods about 16 ± 3 nm in edge length.

If finish injecting in about 10 minutes, the product was a mixture of rods, sheets and spheres with the same major sizes of 15 ± 5 nm. We controlled morphology of Ag nanoparticles by monitoring the position of their major SPR peak using a UV-vis spectrometer. However, this question is still a enigma. We will continue to survey.

REFERENCES

- [1]. S. Jayabal, R Ramaraj, Bimetallic Au/Ag nanorods embedded in functionalized silicate sol-gel matrix as an efficient catalyst for nitrobenzene reduction, *Applied Catalysis A: General* 470 2014, pp. 369– 375
- [2]. K. Bankura, D. Maitya, M. M. R. Mollicka, D. Mondala, B. Bhowmick, I. Roy, T. Midyaa, J. Sarkar, D. Rana, K. Acharya, D. Chattopadhyay, Antibacterial activity of Ag–Au alloy NPs and chemical sensor property of Au NPs synthesized by dextran. *Carbohydrate Polymers* 107 2014, pp.151–157.
- [3]. Y. Wan, Z. Guo, X. Jiang, K. Fang, X. Lu, Y. Zhang, N. Gu, Quasi-spherical silver nanoparticles: Aqueous synthesis and size control by the seed-mediated Lee–Meisel method, *Journal of Colloid and Interface Science* 394 2013: pp. 263–268

- [4]. S. H. Choi, Y. P. Zhang, A. Gopalan, K. P. Lee, H. D. Kang, Preparation of Catalytically Efficient Precious Metallic Colloids by γ -irradiation and Characterization. *Colloids and Surfaces A: Physicochemical and Engineering Aspects* 256 2005: pp. 165 – 170.
- [5]. Z. Li, Y. Li, X. F. Qian, J. Yin, Z. K. Zhu, A Simple Method for Selective Immobilization of Silver Nanoparticles, *Applied Surface Science* 250 2005: pp. 109 – 116.
- [6]. Y. Wang, Y. Zheng, C. Z. Huang, Y. Xia, Synthesis of Ag Nanocubes 18 – 32 nm in Edge Length: The Effects of Polyol on Reduction Kinetics, Size Control, and Reproducibility, *Journal of the American Chemical Society*. 135 2013, pp. 1941 –1951
- [7]. Ratnika Varshney, Seema Bhadauria, Mulayam S.Gaur, Characterization of copper nanoparticles synthesized by a novel microbiological method , *Adv. Mat.Lett.* 1(3), 232 (2010).
- [8]. IA Wani, A Ganguly, J Ahmed, T Ahmad, Silver nanoparticles: ultrasonic wave assisted synthesis, optical characterization and surface area studies, *Mat. Lett.* 65, 520 (2011).
- [9]. Amrut S. Lanje, Satish J. Sharma, Ramchandra B. Pode, Synthesis of silver nanoparticles: a safer alternative to conventional antimicrobial and antibacterial agents, *J. Chem. Pharm. Res.* 2(3), 478 (2010).
- [10]. R. Das, S.S. Nath, D. Chakdar, G. Gope, R. Bhattacharjee, Preparation of Silver Nanoparticles and Their Characterization, *J. of nanotech.* 5, 1 (2009).